Role of NleH, a Type III Secreted Effector from Attaching and Effacing Pathogens, in Colonization of the Bovine, Ovine, and Murine Gut

INFECTION AND IMMUNITY, Nov. 2008, p. 4804–4813 Vol. 76, No. 11
0019-9567/08/$08.00+0 doi:10.1128/IAI.00742-08

Role of NleH, a Type III Secreted Effector from Attaching and Effacing Pathogens, in Colonization of the Bovine, Ovine, and Murine Gut▽

Cordula Hemrajani,[1] Olivier Marches,[1] Siouxsie Wiles,[1] Francis Girard,[1] Alison Dennis,[2] Francis Dziva,[3] Angus Best,[4] Alan D. Phillips,[5] Cedric N. Berger,[1] Aurelie Mousnier,[1] Valerie F. Crepin,[1] Laurens Kruidenier,[6] Martin J. Woodward,[4] Mark P. Stevens,[3] Roberto M. La Ragione,[4] Thomas T. MacDonald,[2] and Gad Frankel[1]*

Division of Cell and Molecular Biology, Imperial College London, London SW7 2AZ, United Kingdom[1]; Institute of Cell and Molecular Science, Barts and the London School of Medicine and Dentistry, London E1 2AT, United Kingdom[2]; Division of Microbiology, Institute for Animal Health, Compton, Newbury, Berkshire RG20 7NN, United Kingdom[3]; Department of Food & Environmental Safety, Veterinary Laboratories Agency (Weybridge), Surrey KT15 3NB, United Kingdom[4]; Centre for Paediatric Gastroenterology, Royal Free Hospital, London, United Kingdom[5]; and Immuno-Inflammation CEDD, GlaxoSmithKline Medicines Research Centre, Stevenage, Hertfordshire SG1 2NY, United Kingdom[6]

Received 12 June 2008/Returned for modification 22 July 2008/Accepted 16 August 2008

The human pathogen enterohemorrhagic *Escherichia coli* (EHEC) O157:H7 colonizes human and animal gut via formation of attaching and effacing lesions. EHEC strains use a type III secretion system to translocate a battery of effector proteins into the mammalian host cell, which subvert diverse signal transduction pathways implicated in actin dynamics, phagocytosis, and innate immunity. The genomes of sequenced EHEC O157:H7 strains contain two copies of the effector protein gene *nleH*, which share 49% sequence similarity with the gene for the *Shigella* effector OspG, recently implicated in inhibition of migration of the transcriptional regulator NF-κB to the nucleus. In this study we investigated the role of NleH during EHEC O157:H7 infection of calves and lambs. We found that while EHEC Δ*nleH* colonized the bovine gut more efficiently than the wild-type strain, in lambs the wild-type strain exhibited a competitive advantage over the mutant during mixed infection. Using the mouse pathogen *Citrobacter rodentium*, which shares many virulence factors with EHEC O157:H7, including NleH, we observed that the wild-type strain exhibited a competitive advantage over the mutant during mixed infection. We found no measurable differences in T-cell infiltration or hyperplasia in colons of mice inoculated with the wild-type or the *nleH* mutant strain. Using NF-κB reporter mice carrying a transgene containing a luciferase reporter driven by three NF-κB response elements, we found that NleH causes an increase in NF-κB activity in the colonic mucosa. Consistent with this, we found that the *nleH* mutant triggered a significantly lower tumor necrosis factor alpha response than the wild-type strain.

The human diarrheal pathogens enteropathogenic *Escherichia coli* (EPEC) and enterohemorrhagic *E. coli* (EHEC) (31) and the murine pathogen *Citrobacter rodentium* (reviewed in reference 28) colonize the host gastrointestinal tract via attaching and effacing (A/E) lesions, which are characterized by intimate adhesion to intestinal epithelia and localized effacement of brush border microvilli (21). EPEC was the first type of *E. coli* to be associated with human disease and is a major cause of infantile diarrhea in developing countries (reviewed in reference 2), while EHEC (O157 and non-O157 strains) is prevalent in developed countries and causes a wide spectrum of illnesses ranging from mild diarrhea to severe diseases such as hemorrhagic colitis and hemolytic uremic syndrome mediated by Shiga toxins (31).

EPEC, EHEC, and *C. rodentium* harbor the locus of enterocyte effacement (LEE) pathogenicity island, which is necessary for A/E lesion formation in vivo (26). The LEE encodes several gene regulators, the outer membrane adhesin intimin (18), the structural components of a type III secretion system (T3SS) (17), chaperones, and translocator and several effector proteins, including Tir (19), Map, EspG, EspF, and EspH (reviewed in reference 12), that are injected into enterocytes via the T3SS and differentially modulate cellular actin dynamics in vitro.

In addition, EPEC, EHEC, and *C. rodentium* use the LEE-encoded T3SS to inject a large number of effectors which are encoded by genes that are scattered around the bacterial genome, carried mainly on prophages and genomic islands (8). Among these effectors are Cif (which causes irreversible cell cycle arrest at the G_2/M transition) (24), EspJ (which is involved in inhibition of receptor-mediated phagocytosis) (23), TccP/$EspF_U$ and TccP2 (which can activate N-WASP) (1, 13, 39), EspI/NleA (which affects exocytosis) (16, 29), and NleH of unknown function (34).

EHEC infection in humans frequently results from direct or indirect contact with ruminant feces; however, the molecular mechanisms underlying colonization of reservoir hosts are ill defined. The LEE-carried genes required for A/E lesion formation (e.g., those for Tir and intimin) play pivotal roles in colonization of such hosts by EHEC O157:H7 (4, 7, 37), and structural components of the T3SS were found by signature-tagged mutagenesis to be required for colonization of calves by EHEC O157:H7 and O26:H− (9, 36). In addition to Tir, EspK

* Corresponding author. Mailing address: Flowers Building, Imperial College, London SW7 2AZ, United Kingdom. Phone: 44 20 7594 5253. Fax: 44 20 7594 3069. E-mail: g.frankel@imperial.ac.uk.
▽ Published ahead of print on 25 August 2008.

TABLE 1. Strains

Species and strain	Characteristics[a]	Source or reference
C. rodentium		
ICC169	Spontaneous Nal^r mutant of wild-type C. rodentium	40
ICC229	ICC169 ΔNleH1 (Kan^r)	This study
ICC180	Bioluminescent strain harboring the *Photorhabdus luxCDABE* operon (Kan^r)	40
ICC285	ICC180 ΔNleH1 (Cm^r)	This study
E. coli		
85-170	Spontaneous Stx1$^-$ and Stx2$^-$ EHEC O157:H7 strain	35
85-170 Nal^r	Spontaneous Nal^r derivative of 85-170	33
ICC232	85-170 Nal^r ΔNleH1ΔNleH2 (Nal^r Kan^r Cm^r)	This study
ICC299	Commensal strain isolated from the cecum of a C57BL/6 mouse	This study

[a] Kan^r, Cm^r, and Nal^r, kanamycin, chloramphenicol, and nalidixic acid resistant, respectively.

TABLE 2. Plasmids

Plasmid	Characteristics	Source or reference
pKD3	*oriRg blaM*; Cm^r cassette flanked by FRT sites	6
pKD4	*oriRg blaM*; Kan^r cassette flanked by FRT sites	6
pKD46	*ori101 repA101*(ts) *araBp-gam-bet-exo blaM*	6
pCP20	FLP synthesis under thermal control	3
pET28-a	His_6 tag expression vector	Novagen
pET:nleH1	Derivative of pET28-a expressing NleH1-His_6	This study
pET:nleH1K159A	Derivative of pET28-a expressing NleH1K159A-His_6	This study

has been shown to influence colonization of the bovine intestine (38), while Map (9), TccP/$EspF_U$ (37), and NleD (25) had no measurable effect. The roles of other T3SS effectors in colonization of ruminants are not known.

C. rodentium is a natural mouse pathogen that, while causing colonic hyperplasia, shares many virulence factors with EPEC and EHEC (reviewed in reference 28). Following inoculation via the oral route, bacteria colonize the colon, typically peaking at day 9 before clearance at around day 17 (27). Recently we refined the *C. rodentium* mouse model by developing noninvasive real-time bioluminescence imaging (BLI) to monitor infection dynamics and tissue tropism in vivo (41). Using this method, we have shown that *C. rodentium* first targets the murine cecal patch and rectum before the infection spreads to the large intestine.

The genome sequences of EHEC O157:H7 strains EDL933 and Sakai, EPEC strain E2348/69, and *C. rodentium* strain ICC168 revealed that EHEC and EPEC contain two *nleH* alleles (34; A. Iguchi et al., unpublished data), while *C. rodentium* harbors only one *nleH* gene. NleH shares 49% sequence similarity with the *Shigella flexneri* T3SS serine/threonine kinase effector protein OspG, which prevents ubiquitination and subsequent degradation of phospho-IκBα and downstream activation of the transcriptional factor NF-κB, possibly via the phosphorylation of the E3 ubiquitin ligase $SCF^{\beta\text{-}TrCP}$ (Skp-Cullin-F box protein) complex (20). NF-κB proteins are transcriptional factors that, when activated, control the transcription of a large number of genes, many of which are involved in the immune (inflammatory) response. The similarities between NleH and OspG prompted us to investigate its role in colonization and activation of the NF-κB pathway in vivo.

MATERIALS AND METHODS

Bacterial strains, plasmids, and primers. The bacterial strains, plasmids, and primers used in this study are described in Tables 1, 2, and 3, respectively. Bacteria were grown at 37°C in Luria-Bertani (LB) broth or agar supplemented with ampicillin (100 μg ml^{-1}), chloramphenicol (25 μg ml^{-1}), kanamycin (50 μg ml^{-1}), and nalidixic acid (Nal) (15 to 25 μg ml^{-1}) as appropriate. *C. rodentium* ICC169 Δ*nleH*, luminescent *C. rodentium* ICC180 Δ*nleH*, and EHEC O157:H7 85-170 Nal^r Δ*nleH1* Δ*nleH2* mutant strains (strains ICC229, ICC285, and ICC232, respectively) were generated using the one-step PCR λ Red-mediated mutation protocol (6) (Table 1). Primers 1 and 2 (Table 3) were used to amplify the kanamycin cassette in pKD4 for deletion of *nleH* in ICC169. Primers 3 and 4 were used to amplify the chloramphenicol cassette in pKD3 for deletion of *nleH* in ICC180. For construction of the EHEC O157:H7 85-170 Nal^r Δ*nleH1* Δ*nleH2* mutant, primers 5 and 6 for *nleH1* and 7 and 8 for *nleH2* were used for amplification of the kanamycin cassette from pKD4. Prior to deletion of *nleH1* from 85-170 Δ*nleH2*, the kanamycin cassette was deleted as described previously (6) using the pCP20 vector (3).

The PCR product of the resistance cassette, flanked by approximately 50 bp of *nleH*, was digested with DpnI and the cassette electroporated into the recipient strains carrying pKD46, encoding the λ Red recombinase. Mutants were selected on selective LB plates with kanamycin or chloramphenicol. Recombinant clones were cured of pKD46 and the mutation confirmed by PCR using primers flanking *nleH* and primers within the antibiotic resistance gene. Growth curves have confirmed that the mutant and wild-type stains have identical growth rates in LB and minimal media. Mutations of the *nleH1* and *nleH2* genes created using the same method in EPEC strains were successfully complemented in *trans* during in vitro studies.

Oral inoculation of calves. All animal experiments were performed in accordance with the Animals (Scientific Procedures) Act 1986 and were approved by the local Ethical Review Committee. Groups of four 12-day-old Friesian bull calves were separately inoculated with approximately 10^{10} CFU of wild-type 85-170 Nal^r or 85-170 Nal^r Δ*nleH1* Δ*nleH2* as described previously by Stevens et al. (33). The magnitude and duration of fecal excretion of the bacteria were followed daily for 14 days. Wild-type and mutant bacteria were enumerated by plating of triplicate serial dilutions of fresh feces collected by rectal palpation onto sorbitol-MacConkey agar supplemented with potassium tellurite (2.5 mg ml^{-1}) (T-SMAC) containing 25 μg ml^{-1} Nal (T-SMAC-Nal) and onto T-SMAC-Nal containing 50 μg ml^{-1} kanamycin, respectively. Recovery of wild-type and mutant bacteria was confirmed by PCR from selected colonies using *nleH*-flanking primers. The sensitivity of detection was 10^2 CFU/g. Fecal excretion data were statistically analyzed for the effect of mutation by means of an F test, with the data taken as repeated measurements and the animal as a covariant (Proc Mixed, Statistical Analysis System 1995; SAS Institute, Cary, NC). *P* values of <0.05 were considered significant.

Oral inoculation of lambs. Fifteen 6-week-old crossbred lambs were randomly divided into three equal groups, supplied with food and water ad libitum, and confirmed to be free of *E. coli* O157:H7 by enrichment and O157 immunomagnetic separation. All lambs were housed in biosecure containment level 2 accommodations. Each group was housed in a separate room with its own air handling. The animals were visited by experienced staff, who changed protective clothing between groups. Five lambs were each dosed orally with 10^9 CFU of either wild-type 85-170 Nal^r or the isogenic Δ*nleH1* Δ*nleH2* mutant separately, or with wild-type 85-170 Nal^r and the Δ*nleH1* Δ*nleH2* mutant together, suspended in 10 ml of 0.1 M phosphate-buffered saline (PBS) (pH 7.4). Approximately 24 h after oral inoculation and as required thereafter for up to 28 days, rectal fecal samples from each lamb were collected for direct plating onto SMAC supplemented with either 15 μg of Nal/ml or 25 μg of kanamycin/ml. Samples that were O157 negative on direct plating were enriched in buffered peptone water for 6 h at 37°C and then plated onto SMAC plates supplemented with the appropriate

TABLE 3. Primers

Primer no.	Primer name	Sequence (5′→3′)
1	NleH CRICC169 Fw	ATGTTATCACCAGCTCCTGTAAATTTGGGATGTTCATGGAATTCTT TAACTGTGTAGGCTGGAGCTGCTTCG
2	NleH CRICC169 Rv	AATTCTACTTAATACCACTCTGATAAGATCTTGCTTTCCTCCATGA TAAGCATATGAATATCCTCCTTAG
3	NleH CRICC180 Fw	ATGTTATCACCAGCTCCTGTAAATTTGGGATGTTCATGGAATTCTT TAACGTATACTTATAGGAGGAATC
4	NleH CRICC180 Rv	TTAAATTCTACTTAATACCACTCTGATAAGATCTTGCTTTCCTCCAT GATACACATCCGACCTCGACGAAGC
5	NleH1 EHEC Fw	TGAAGGTTGAAATGTATGTTATCGCCATATTCTGTAAATTTGGGA TGTTCTGTGTAGGCTGGAGCTGCTTCG
6	NleH1 EHEC Rv	CACTACACTGGATAAAATTACTAAATTTTACTTAATACCACACTAA TAAGCATATGAATATCCTCCTTAG
7	NleH2 EHEC Fw	ATGTTATCGCCCTCTTCTATAAATTTGGGATGTTCATGGAATTCTT TAACGTGTAGGCTGGAGCTGCTTC
8	NleH1 EHEC Rv	TATCTTACTTAATACTACACTAATAAGATCCAGCTTTCCTCCGTGA TAAGCATATGAATATCCTCCTTA
9	TNF-α-Fw	ATGAGCACAGAAAGCATGATC
10	TNF-α-Rv	TACAGGCTTGTCACTCGAATT
11	B-actin-Fw	AGAGGGAAATCGTGCGTGAC
12	B-actin-Rv	CAATAGTGATGACCTGGCCGT
13	IFN-γ-Fw	TGAACGCTACACACTGCATCTTGG
14	IFN-γ-Rv	CGACTCCTTTTCCGCCTTCCTGAG

antibiotic. Representative colonies were confirmed to be *E. coli* O157 by latex agglutination (Oxoid). For coinfection studies, the competitive index (CI) was calculated; it is defined as the ratio between the mutant and wild-type strains within the output (bacteria recovered from the host after infection) divided by their ratio within the input (initial inoculum). For this experiment, the input ratio was 1:1. The null hypothesis that CI = 1 was tested by a two-sided *t* test.

Murine models. Specific-pathogen-free female 6- to 8-week-old mice were used in this study. Wild-type inbred C57BL/6 and DBA-1 mice were purchased from Harlan UK Ltd. (Bicester, United Kingdom), while the transgenic light-producing animal model DBA-1 NF-κB-luc (Oslo) (P/N 119335) was purchased from Xenogen-Caliper Corp. (Alameda, CA). The transgenic light-producing animal model NF-κB-RE-luc (Oslo)-Xen, commonly called NF-κB-RE-luc (Oslo), carries a transgene containing three NF-κB responsive-element (RE) sites from the immunoglobulin κ light-chain promoter and modified firefly luciferase cDNA. All animals were housed in individually HEPA-filtered cages with sterile bedding and free access to sterilized food and water. Independent experiments were performed at least twice (but only once for histology) using at least four mice per group.

Oral infection of mice, harvesting and collection of tissues, and bacterial stool counts. Mice were orally inoculated using a gavage needle with 200 μl of overnight LB-grown bacterial suspension in PBS (~5×10^9 CFU). The number of viable bacteria used as the inoculum was determined by retrospective plating onto LB agar containing antibiotics. Stool samples were recovered aseptically at various time points after inoculation and the number of viable bacteria per gram of stool determined after homogenization at 0.1g ml^{-1} in PBS and plating onto LB agar containing the appropriate antibiotics. At selected time intervals postinfection, blood was collected by cardiac puncture and mice were sacrificed by cervical dislocation. Sections of distal colon were collected and snap frozen in liquid nitrogen before storage at −70°C prior to analysis. For coinfection studies, the CI was calculated as described previously by Mundy et al. (30). For this experiment, the input ratio of wild-type strain to mutant strain was approximately 1:2. The null hypothesis that CI = 1 was tested by a nonparametric Wilcoxon two-tailed test using the GraphPad InStat software (GraphPad Software Inc., San Diego, CA).

In vivo BLI. Prior to imaging, the abdominal region of each mouse was depilated to minimize any potential signal impedance by melanin within pigmented skin and fur. Bioluminescence (photons s^{-1} cm^{-2} sr^{-1}) from living infected animals was measured after gaseous anesthesia with isofluorane using the IVIS50 camera system (Xenogen-Caliper Corp., Alameda, CA). The sample shelf was set to position D (field of view, 15 cm). A photograph (reference image) was taken under low illumination prior to quantification of photons emitted from strain ICC180 at a binning of 4 over 1 to 10 min using the software program Living Image (Xenogen-Caliper Corp.) as an overlay on Igor (Wavemetrics, Seattle, WA). For anatomical localization, a pseudocolor image representing light intensity (from blue [least intense] to red [most intense]) was generated using the Living Image software and superimposed over the gray-scale reference image. Bioluminescence within specific regions of individual mice was also quantified using the region-of-interest tool in the Living Image software program (given as photons s^{-1}). For expression of light from the NF-κB reporter mice, 180 mg kg^{-1} D-luciferin (Gold Biotechnology, St. Louis, MO) dissolved in 250 μl PBS (pH 7.8) was administered by intraperitoneal injection 5 min prior to imaging. As a positive control for luciferase gene expression from the NF-κB-RE-luc (Oslo) mice, tumor necrosis factor alpha (TNF-α) (2 μg per mouse) was administered by intraperitoneal injection.

Histopathology. Segments of the cecum and the terminal colon of each mouse were collected at 9 and 14 days postinoculation, rinsed of their content, and fixed in 10% buffered formalin for microscopic examination. Formalin-fixed tissues were then processed, paraffin embedded, sectioned at 5 μm, and stained with hematoxylin and eosin (H&E) according to standard techniques. Sections were examined by light microscopy for the presence of intimately adhering bacteria on intestinal cells, as previously described (15). Crypt length was also evaluated, and the lengths of at least four well-oriented crypts were measured for each section. A nonparametric analysis of variance (ANOVA) with a posteriori comparisons was performed using commercially available GraphPad InStat v3.06 software (GraphPad Software Inc., San Diego, CA). *P* values of ≤0.05 were considered significant.

Immunohistochemistry. Snap-frozen colonic tissues, embedded in OCT mounting medium (VWR BDH, Lutterworth, United Kingdom), were sectioned using a cryostat to a thickness of 5 μm. Sections were mounted on polysine slides (VWR BDH) and air dried overnight before fixing in acetone at room temperature for 20 min. After air drying for 1 h, sections were rehydrated in Tris-buffered saline (TBS) for 5 min and then incubated with antibodies against CD3, CD4, and CD8 (Serotec, Oxford, United Kingdom) at a dilution of 1:50 to 1:100 for 1 h. Sections were gently washed with TBS three times before addition of biotinylated anti-rat immunoglobulin G (Serotec) at a dilution of 1:200 with 4% (vol/vol) normal murine serum for blocking (Sera Laboratories International, Horsted Keynes, United Kingdom) for 30 min. After washing, a 1:200 dilution of 0.1% avidin-peroxidase (Sigma-Aldrich, Dorset, United Kingdom) was added and left for 30 min before further washing and treatment with diaminobenzadine substrate (Sigma-Aldrich) for 5 min. The reaction was stopped with excess TBS, and sections were counterstained with Mayer's hematoxylin (Sigma-Aldrich) for 30 s, dipped in acid alcohol, and washed in tap water for 5 min. Sections were dehydrated through an ethanol gradient of 70%, 90%, and 100% solutions (2 min each), followed by clearing in Histoclear (VWR BDH) and mounting in DPX (VWR BDH). A control slide using no primary antibody was also made to show endogenous peroxidase-containing cells. Stained cell populations were counted in five randomly selected fields per section, and data were expressed as the number of T cells per 250 μm^2 of lamina propria.

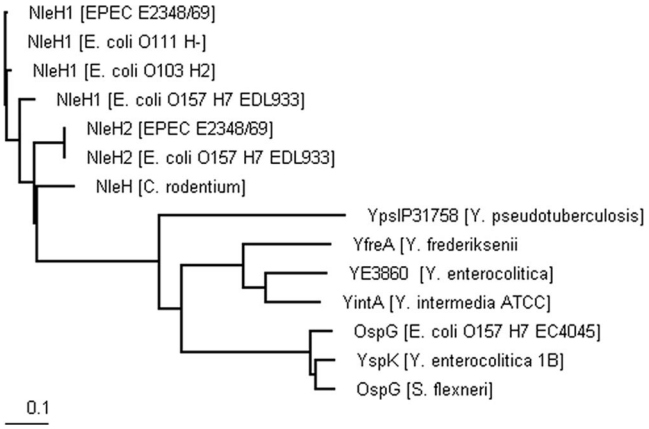

FIG. 1. Distance tree of the NleH family. Homologues were identified using BLASTp searches of NCBI nr protein database with EPEC 2348/69 NleH1 as the query sequence. Protein sequences selected and analyzed included *E. coli* O111:H− NleH1 (GI:164457622), *E. coli* O103:H2 NleH1 (GI:164457632), *E. coli* O157:H7 EDL933 NleH2 (GI:15801938), *C. rodentium* NleH (GI:44888794), phage cdtI gp23 (GI:148609405), *Y. pseudotuberculosis* IP 31758 (GI:153930640), *Y. frederiksenii* ATCC 33641 YfreA (GI:77972806), *Y. enterocolitica* subsp. *enterocolitica* 8081 (GI:123442682), *Y. intermedia* ATCC 29909 YintA (GI:77977119), *Y. enterocolitica* subsp *enterocolitica* 8081 YspK (GI:13442682), *S. flexneri* OspG (GI:13449175), and *E. coli* O157:H7 str EC4045 OspG (GI:168711271), as well as EPEC 2348/69 NleH2 (unpublished). The BioEdit software was used to create a ClustalW alignment. Clustal W2 (EMBL-EBI ebi.ac.uk) was used to create a phylogram, and TreeView (Bioedit) was used for visualization.

SEM. Intestinal segments were fixed in 2.5% glutaraldehyde and processed for scanning electron microscopy (SEM) as previously described (14). SEM samples were examined blindly at 25 kV using a JEOL JSM-5300 SEM [JEOL (UK) Ltd., Herts, United Kingdom].

IFA. An indirect immunofluorescence assay (IFA) was used for the detection of *C. rodentium* (serotype O152) in formalin-fixed, paraffin-embedded sections as previously described (14). Tetramethyl rhodamine isothiocyanate-conjugated donkey anti-rabbit (Jackson ImmunoResearch Europe Ltd., Soham, Cambridgeshire, United Kingdom) secondary antibody was used to visualize O152-positive bacteria, while DNA of both bacteria and epithelial cells was counterstained with Hoechst 33342 (Sigma-Aldrich Co., United Kingdom). Sections were examined with an Axio Imager M1 microscope (Carl Zeiss MicroImaging GmbH, Germany). Images were acquired using an AxioCam MRm monochrome camera and computer processed using AxioVision (Carl Zeiss MicroImaging GmbH, Germany) and Adobe Photoshop 5.0 and Adobe Illustrator 8.0 software (Adobe Systems Incorporated, CA).

RNA extraction and quantitative RT-PCR. Total RNA was isolated from frozen colonic tissue using the RNeasy Plus minikit (Qiagen). All tissues used were harvested from mice 14 days after oral gavage. Total RNA was measured using a Nanodrop. TNF-α or gamma interferon (IFN-γ) and β-actin mRNAs were measured by semiquantitative reverse transcription-PCR (RT-PCR) using primers 9 to 14 listed in Table 3 and the one-step Reverse-iT hot-start kit (Thermo). The PCR amplification cycle was 20 s at 94°C, 30 s at 60°C, and 60 s at 72°C for 35 cycles. One microgram of RNA was used for measurement of TNF-α and IFN-γ transcript levels, and 100 ng of RNA was used for detection of β-actin mRNA. The PCR products were run on a 1% agarose gel alongside the 100-bp ladder from NEB in Tris-borate-EDTA buffer. GeneTools (Syngene) was used to conduct densitometric analysis. All TNF-α/β-actin and IFN-γ/β-actin ratios were compared between mice infected with wild-type and *nleH* mutant bacteria. Statistical analyses were conducted with the one-way ANOVA Bonferroni multiple-comparison test using the GraphPad InStat software (GraphPad Software Inc., San Diego, CA), as all groups displayed normal distributions.

RESULTS

The NleH T3SS effector homologues. NleH belongs to a family of T3SS effectors found in diverse enteric pathogens.

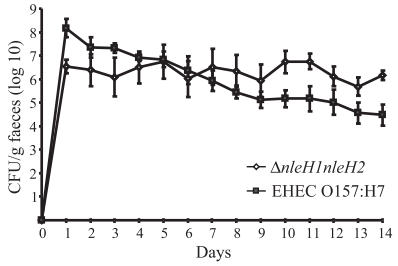

FIG. 2. Course of fecal excretion of EHEC O157:H7 following oral challenge of 12-day-old calves with wild-type strain 85-170 Nal^r or the 85-170 Nal^r Δ*nleH1* Δ*nleH2* mutant. Data represent the mean daily fecal count (n = 4 per strain) ± standard error of the mean.

EPEC O127:H6 E2348/69 and EHEC O157:H7 EDL933 and Sakai contain two NleH paralogues, which share 83 to 84% protein identity. *C. rodentium* contains only one *nleH* gene, which shares 83 and 81% amino acid sequence identity with EHEC O157:H7 NleH1 and NleH2, respectively. NleH shares 49% amino acid sequence similarity with the serine/threonine kinases OspG and YspK (*Yersinia* secreted protein kinase) of *Yersinia enterocolitica.*

We employed BLASTp searches of the NCBI protein database using EPEC E2348/69 NleH1 as the query sequence. The Clustal W2 software (EMBL-EBI) was then used to create a phylogram of the different homologues (Fig. 1). Two major clusters were formed, one containing all the NleH effectors and the other containing closer homologues of OspG, including an OspG-like effector (90.8% identity to OspG of *Shigella*) from

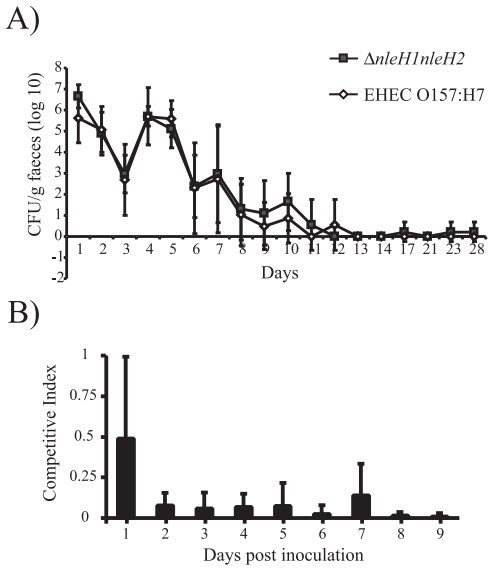

FIG. 3. (A) Course of fecal excretion of EHEC O157:H7 following oral challenge of 6-week-old lambs with wild-type strain 85-170 Nal^r or the 85-170 Nal^r Δ*nleH1* Δ*nleH2* mutant. Data represent the mean daily fecal count (n = 5 per strain) ± standard error of the mean. (B) CI of EHEC O157: H7 85-170 Nal^r Δ*nleH1* Δ*nleH2* in lambs infected with an inoculum containing a 1:1 ratio of wild-type EHEC and the Δ*nleH1* Δ*nleH2* double mutant. The null hypothesis that CI = 1 was tested by a two-sided t test and shows that the mean CI postchallenge is significantly less than 1 for all time points where it could be calculated except day 1.

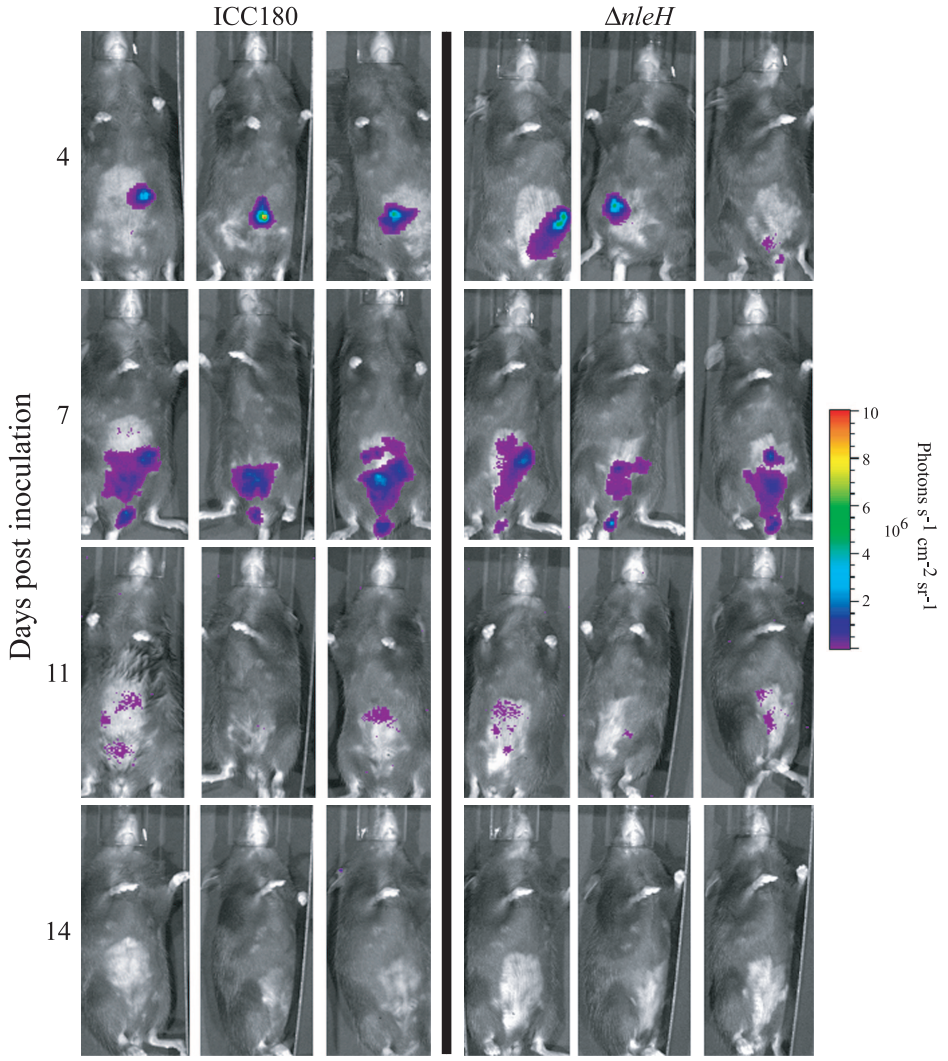

FIG. 4. Anatomical localization of luminescent wild-type *C. rodentium* ICC180 and Δ*nleH* strains during in vivo infection of mice. Images were acquired using an IVIS50 system and displayed as pseudocolor images of bioluminescence. The variations in color represent light intensity at a given location, with red being the most intense light emission and blue being the weakest signal. The colored scale to the right indicates relative signal intensity in photons $s^{-1}cm^{-2}$ sr^{-1}. At each time point postgavage, mice were imaged with an integration time of 1 min.

EHEC O157:H7 strain EC4045. To determine the role of NleH proteins in vivo, we generated EHEC O157:H7 (strain 85-170) Δ*nleH1* Δ*nleH2* and *C. rodentium* (ICC169 and bioluminescent strain ICC180) Δ*nleH* mutants.

The EHEC O157:H7 Δ*nleH1* Δ*nleH2* double mutant is shed in greater numbers than the parental strain from orally challenged calves. To assess the role of NleH in intestinal colonization of calves by EHEC O157:H7, wild-type and mutant bacteria were separately inoculated into four 12-day-old Friesian bull calves. Both wild-type and mutant strains colonized the calves efficiently, and the mutant was excreted at lower levels than the wild type during the first 4 days. From day 7 the mutant was shed at higher levels than the wild-type strain, and the difference became statistically significant ($P < 0.05$) from day 10 onwards (Fig. 2). The course of the fecal excretion of the wild-type strain was consistent with previously observed patterns (10, 33, 37).

Contribution of NleH1 and NleH2 to colonization of conventional 6-week-old-lambs. A 6-week-old lamb model was next used to compare the persistence of an *E. coli* O157:H7 Δ*nleH1* Δ*nleH2* double mutant and the isogenic wild-type strain. The ability of the mutant to establish itself and persist in lambs was investigated by monitoring the viable counts recovered in fecal pellets collected per animal. When given as a single inoculum, the wild-type *E. coli* O157:H7 isolate produced the classical shedding pattern in lambs, as described previously (5, 42), persisting in relatively high numbers during the early stages of infection and then declining by day 11 postinoculation (Fig. 3A). The Δ*nleH1* Δ*nleH2* mutant demonstrated a similar shedding pattern, except that positive fecal samples were noted only until day 12 postinoculation (Fig. 3A). When both isolates were administered in the same inoculum, the wild type persisted for 4 days longer than the Δ*nleH1* Δ*nleH2* mutant (data not shown). The mean CI was signifi-

cantly less than 1 for all time points where it could be calculated except day 1 (Fig. 3B), demonstrating that the wild-type strain outcompeted the Δ*nleH1* Δ*nleH2* mutant in the ovine model.

Contribution of NleH to colonization in the *C. rodentium* murine model. We followed the anatomical localization and pathogenic burden using BLI and viable counts in stools of mice infected with either wild-type or Δ*nleH C. rodentium*. Using BLI, we observed that both the wild-type and mutant strains colonized the cecal patch and rectum by day 3 to 4 postinfection. After adaptation to the in vivo environment (day 6 to 7), the entire distal colon was then heavily infected. Clearance began by day 10, at which point light intensity decreased. By day 14 the gastrointestinal tract had mostly cleared the infection (Fig. 4). Viable counts of bacteria in stool mirrored the results obtained by BLI; no significant differences in viable bacterial counts of the wild-type and Δ*nleH* mutant strains were seen (Fig. 5A). However, the Δ*nleH C. rodentium* mutant was significantly out competed by the wild-type strain in a mixed infection (Fig. 5B).

NleH does not affect A/E lesion formation and T-cell infiltration in the *C. rodentium* murine model. The hallmarks of *C. rodentium* infection include induction of extensive colonic hyperplasia and influx of T cells into the colonic lamina propria. Histological examination and measurement of crypt length did not reveal any differences between the parent and mutant strains (data not shown). Immunohistochemistry, performed to investigate the influx of $CD3^+$, $CD4^+$, and $CD8^+$ T cell subsets into the colonic lamina propria at 14 days postinoculation, revealed that although the Δ*nleH* mutant-infected animals showed slightly fewer CD3- and CD4-positive T cells in the lamina propria, no significant differences were observed between animals infected with the mutant or wild-type *C. rodentium* strains (data not shown). Immunofluorescent staining with anti-O152 and SEM analysis at day 9 or day 14 postinoculation did not reveal any differences between the wild-type and Δ*nleH C. rodentium* strains (Fig. 6).

NleH influences NF-κB levels and expression of TNF-α in vivo. A recent study has shown that OspG inhibits degradation of IκB and hence activation of NF-κB and that a *Shigella ospG* mutant induces a stronger inflammatory response than the wild-type strain after inoculation of rabbit ileal loops (20). In order to determine if NleH influences activation of NF-κB in vivo, we infected NF-κB-RE-luc reporter mice with *C. rodentium* wild-type strain ICC169 or ICC169 Δ*nleH*; mice inoculated with the commensal *E. coli* strain ICC299 (Table 1) or PBS were used as controls. The number of *nleH* mutant bacteria shed from this mouse strain was similar to that of the wild type (data not shown). No significant differences in whole-body (including chest, neck, abdomen, and rectum) luminescence counts were recorded by live imaging, at any time point, between PBS-gavaged animals and those gavaged with wild-type *C. rodentium*, the *nleH* mutant, or the commensal *E. coli.* On day 14 postchallenge, we recorded luminescence counts in different organs. While no significant difference in the luminescence counts was seen in the mesenteric lymph nodes, spleens, and ceca of the different mouse groups (Table 4), there was a significant ($P = 0.0024$) 2.5-fold increase in the signal from the colon in mice infected with the wild-type *C. rodentium* compared to those inoculated with *C. rodentium*

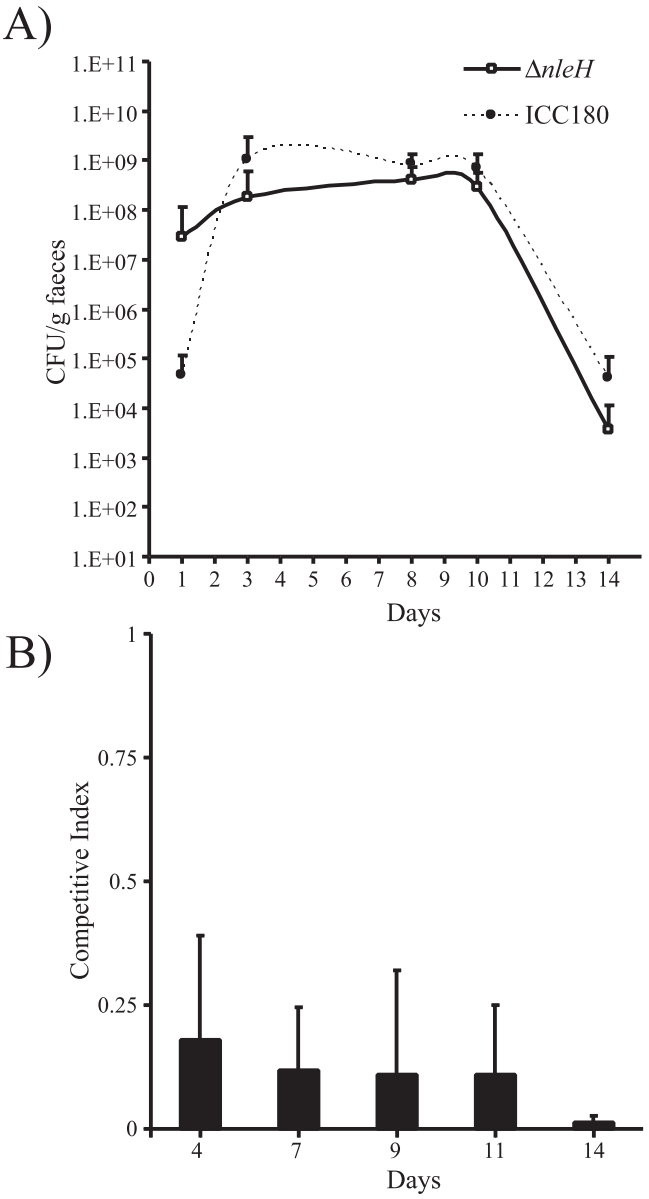

FIG. 5. (A) Course of fecal excretion following oral challenge of groups of six 6- to 8-week-old C57BL/6 mice with either wild-type *C. rodentium* ICC180 or the Δ*nleH* mutant. (B) Mean CI of *C. rodentium* Δ*nleH* in mice infected with an inoculum containing a 1:2 ratio of wild-type *C. rodentium* and the Δ*nleH* mutant. The null hypothesis that CI = 1 was tested by a two-tailed nonparametric Wilcoxon test and showed that the mean CI postchallenge is significantly less than 1 for all time points where it could be calculated.

Δ*nleH*, *E. coli* ICC299, or PBS (Fig. 7A and B). This difference was similar to the three- to fourfold-increased luminescent signal seen after mice were inoculated with TNF-α as a positive control (data not shown).

As NF-κB induces the transcription of many proinflammatory cytokines such as TNF-α and IFN-γ, we compared the levels of their transcripts in uninfected mice and mice infected with either wild-type or Δ*nleH* mutant *C. rodentium*. RNA extracted from distal colons of mice was subjected to semiquantitative RT-PCR. Transcript levels were quantified as a

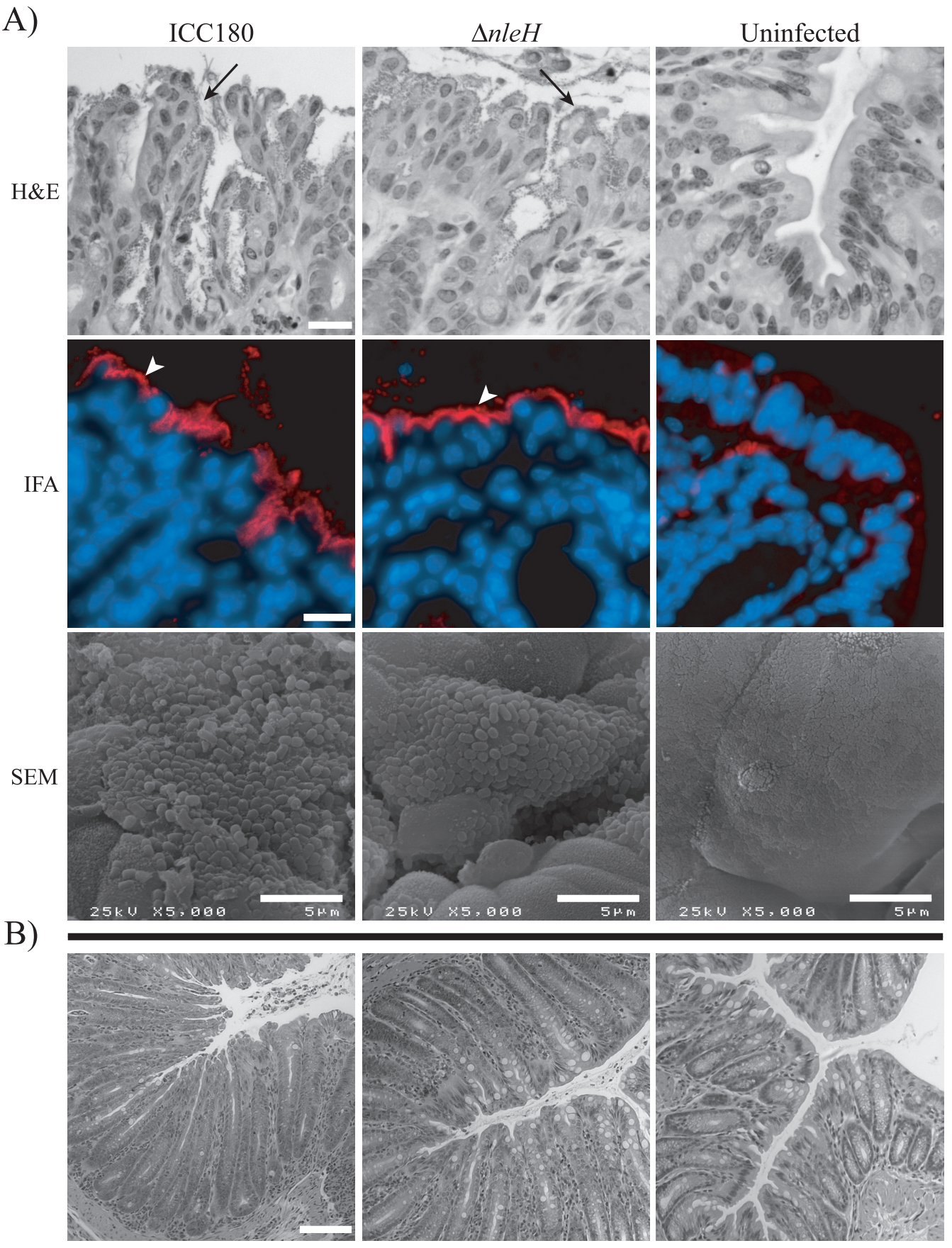
A)
ICC180
ΔnleH
Uninfected
H&E
IFA
SEM
25kV X5,000 5μm
25kV X5,000 5μm
25kV X5,000 5μm
B)

TABLE 4. Specific bioluminescence from each organ at harvest

Inoculum	Specific bioluminescence (mean ± SD) from:				
	Cecum	Mesenteric lymph nodes	Spleen	Colon	Intestines
ICC169	$2.59 \times 10^5 \pm 8.00 \times 10^4$	$2.35 \times 10^6 \pm 9.47 \times 10^5$	$9.25 \times 10^4 \pm 2.29 \times 10^4$	$1.41 \times 10^6 \pm 2.92 \times 10^5$	$1.72 \times 10^6 \pm 4.69 \times 10^5$
Δ*nleH* mutant	$1.80 \times 10^5 \pm 9.89 \times 10^4$	$2.75 \times 10^6 \pm 1.26 \times 10^6$	$2.12 \times 10^5 \pm 2.38 \times 10^5$	$5.69 \times 10^5 \pm 2.53 \times 10^5$	$2.08 \times 10^6 \pm 1.04 \times 10^6$
PBS	$3.61 \times 10^5 \pm 8.78 \times 10^4$	$3.02 \times 10^6 \pm 8.61 \times 10^5$	$8.33 \times 10^4 \pm 1.71 \times 10^4$	$6.34 \times 10^5 \pm 2.37 \times 10^5$	$1.53 \times 10^6 \pm 6.35 \times 10^5$
Commensal strain	$2.69 \times 10^5 \pm 4.42 \times 10^4$	$2.58 \times 10^6 \pm 8.11 \times 10^5$	$1.39 \times 10^5 \pm 2.81 \times 10^4$	$5.02 \times 10^5 \pm 1.03 \times 10^5$	$2.38 \times 10^6 \pm 4.27 \times 10^5$

ratio of TNF-α or IFN-γ to β-actin. This revealed that the levels of TNF-α mRNA were significantly higher in tissues extracted from infected mice than in those from uninfected control mice. Mice infected with the wild-type *C. rodentium* had significantly higher TNF-α transcript levels than those infected with the Δ*nleH* mutant (Fig. 8). The levels of IFN-γ transcript were comparable in all mouse groups (data not shown).

DISCUSSION

Many gram-negative bacterial pathogens use T3SS effectors to modulate host cell signaling pathways. Effector proteins can trigger local (e.g., alteration in the cytoskeleton) or systemic (e.g., immune response) changes. Colonization of the mucosal surface requires temporal modulation of the host immune status. While downregulation of innate immunity might aid the pathogen to launch an infection and to reach a critical mass, activation of the immune system might assist the pathogen in its competition with the resident gut microflora. It is therefore not surprising that pathogenic bacteria are equipped with virulence factors which have antagonistic immune modulation activities. Indeed, in a recent report Lupp et al. demonstrated that *C. rodentium* population expansion in vivo is mediated by an inflammatory response that disrupts the endogenous intestinal microbiota (22). In contrast, using polarized culture models, Ruchaud-Sparagano et al. have shown that EPEC inactivates innate immune responses in vitro (32).

In this study we investigated the role of NleH in colonization, competitiveness, and activation of the NF-κB pathway in vivo. EPEC O127:H6 E2348/69 and EHEC O157:H7 EDL933 and Sakai contain two, almost identical, copies of *nleH*, while *C. rodentium* harbors only a single *nleH* gene. The functional consequences of this gene duplication are not known. Interestingly, a recent shotgun sequencing of a number of EHEC O157:H7 isolates has shown that they contain, in addition to *nleH*, a gene whose product shares 90.8% sequence identity with OspG (NCBI BLASTp).

Investigation of the contribution of NleH toward colonization and competitiveness of EHEC O157:H7 in bovine and ovine hosts, which are important animal reservoirs of the pathogen, showed that the EHEC O157 Δ*nleH1* Δ*nleH2* double mutant was shed in greater numbers than the parental strain from orally challenged calves, significantly from day 10 postinoculation. The precise effect of deleting *nleH* on factors or regulatory mechanisms involved in EHEC O157:H7 colonization in bovine intestines remains to be investigated. In single-infection studies with lambs, there was no statistical difference in shedding after oral inoculation with the same strains. However, CIs measured following oral inoculation of lambs with a mixture of wild-type EHEC O157:H7 and the Δ*nleH1* Δ*nleH2* double mutant revealed that the mutant was significantly outcompeted. The reasons for the different phenotypes observed in the bovine and ovine models are currently not known. However, these results show that effector proteins might have dissimilar or even opposite functions in different hosts.

In order to determine the contribution of NleH to infection with *C. rodentium*, we mutated *nleH* in the wild-type ICC169 and luminescent ICC180 strains. Deletion of *nleH* from *C. rodentium* had no significant effect on in vivo tissue tropism, bacterial burden, colonic hyperplasia, or infiltration of $CD3^+$, $CD4^+$, and $CD8^+$ cells to the lamina propria. A subtle phenotype was recently reported for *C. rodentium* Δ*nleH* in single infection, as expansion of the mutant population in vivo lagged behind that of the wild-type population during early stages (6 days postchallenge), although at later stages (10 days) the mutant and wild type colonized at comparable levels (11). The reasons for the different results might be due to the mouse status (i.e., composition of the normal gut flora), preparation of the inocula, or bacterial strains. Importantly, we found that in a mixed infection the *nleH* mutant was significantly outcompeted by the wild-type strain, suggesting that expression of NleH increases the bacterial fitness in vivo. This could explain the need for conservation and multiplicity of the gene in EHEC and EPEC strains.

As we did not observe any difference in colonization and clearance dynamics, hyperplasia, and T-cell infiltration between the wild-type and Δ*nleH* mutant strains, NleH appears to have a local rather than systemic role, possibly in displacing

FIG. 6. Interaction of wild-type *C. rodentium* strain ICC180 and its Δ*nleH* mutant with the colonic epithelium in vivo. (A) At day 9 postchallenge, typical foci of intimately adherent bacteria (arrows) were observed on H&E-stained sections, accompanied by a highly disorganized epithelium. IFA staining revealed these bacteria to be of the O152 serotype (arrowheads), corresponding to *C. rodentium* serotype. These foci of intimately adherent bacteria were confirmed to be A/E lesions by SEM. Neither O152-positive bacteria nor A/E lesions were observed on sections or samples derived from uninfected mice. (B) No adherent bacteria were observed in the colons of mice infected with ICC180 and the ICC180 Δ*nleH* mutant at day 14 postchallenge, although crypt hyperplasia was still present. For the IFA panel: Hoechst 33342 (blue, false color), DNA; tetramethyl rhodamine isothiocyanate (intense blue, false color), O152-positive bacteria. Representative micrographs are shown. Bar, 20 μm (H&E and IFA) or 100 μm (B).

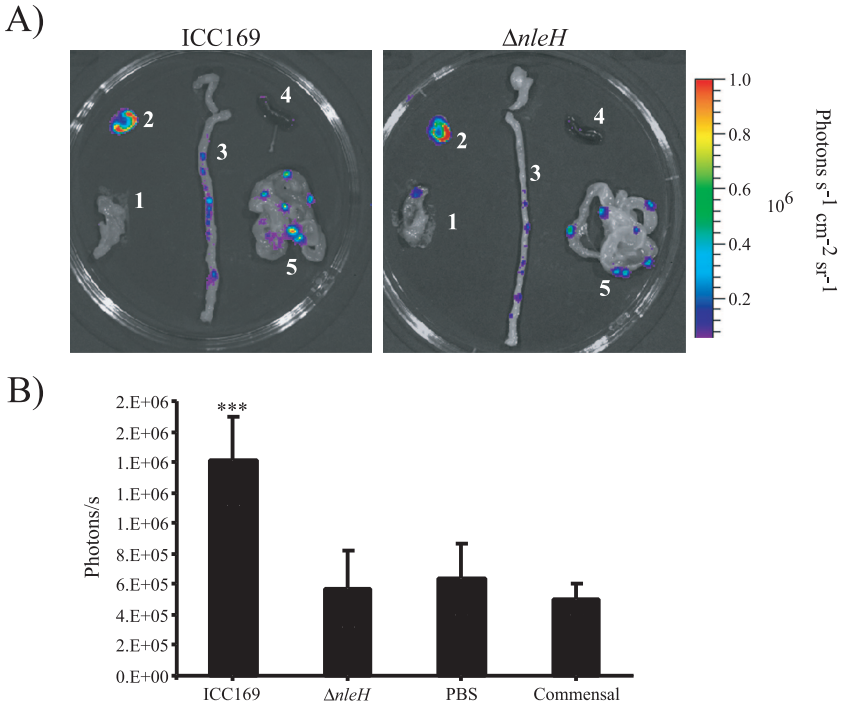

FIG. 7. NF-κB activation in organs of mice at 14 days postchallenge. Luminescence was measured in extracted organs. NF-κB-RE-luc reporter mice were inoculated with wild-type (strain ICC169) or Δ*nleH C. rodentium.* (A) Representative bioluminescence images captured using the IVIS50 camera system are shown (cecum [1], mesenteric lymph nodes [2], colon [3], spleen [4], and intestine [5]. Luminescence was quantified using the region-of-interest tool in the Living Image software (given as photons s^{-1}). (B) Graph of luminescence in extracted colons shows a significant loss of NF-κB activation in the absence of *nleH*. ***, $P < 0.005$.

the normal gut flora. Considering that both NleH (C. Hemrajani, unpublished data) and OspG (20) are protein kinases and share a high level of sequence identity, we investigated, using reporter mice, if NleH plays a role in activation of the NF-κB pathway. Unexpectedly, we found lower activation of NF-κB in the colon in mice infected with the *C. rodentium* Δ*nleH* mutant than in those infected with the parental wild-type strain. Consistent with these results, we found lower colonic levels of TNF-α at 14 days postchallenge in mice infected with the Δ*nleH C. rodentium* mutant than in those infected with the wild-type strain, while no difference was recorded for IFN-γ. These data suggest that NleH triggers local activation of NF-κB, which in turn leads to a differential increase in the levels of proinflammatory cytokines.

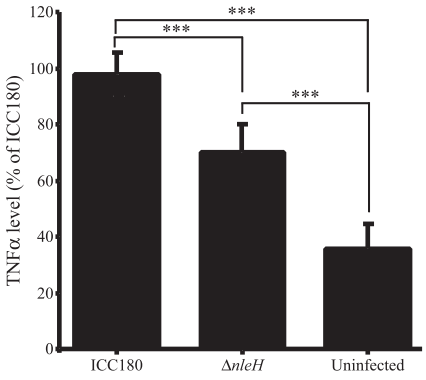

FIG. 8. Semiquantitative TNF-α and β-actin RT-PCRs were performed on RNA isolated from colons of uninfected mice or mice orally challenged with wild-type or Δ*nleH C. rodentium*. Median TNF-α levels (measured as a ratio of TNF-α to β-actin) in *C. rodentium*-infected mice were considered the basal level of activation by wild-type bacteria in each experiment and taken as 100%. All TNF-α/β-actin ratios were compared to this and expressed as a percentage of the median TNF-α level during wild-type infection. GeneTools (Syngene) was used for densitometric analysis. Two repetitions, each using four or five mice per group, were conducted and graphed. The one-way ANOVA Bonferroni multiple-comparison test was used to determine significance, as the three groups had normal distributions. ***, $P < 0.001$.

Collectively these results demonstrate that the role of NleH during infection is host specific. NleH, one of the core and conserved T3SS effectors in A/E pathogens, is likely to work with other effectors in optimizing the level of local gut inflammatory responses and the relationship with the endogenous gut flora for the benefit of the pathogen.

ACKNOWLEDGMENTS

We thank Robin Sayers (VLA) for the statistical analysis of the ovine data.

This work was supported by grants from the MRC and the Wellcome Trust.

REFERENCES

1. **Campellone, K. G., D. Robbins, and J. M. Leong.** 2004. EspFU is a translocated EHEC effector that interacts with Tir and N-WASP and promotes Nck-independent actin assembly. Dev. Cell **7:**217–228.
2. **Chen, H. D., and G. Frankel.** 2005. Enteropathogenic *Escherichia coli*: unravelling pathogenesis. FEMS Microbiol. Rev. **29:**83–98.
3. **Cherepanov, P. P., and W. Wackernagel.** 1995. Gene disruption in *Escherichia coli*: TcR and KmR cassettes with the option of Flp-catalyzed excision of the antibiotic-resistance determinant. Gene **158:**9–14.

4. **Cornick, N. A., S. L. Booher, and H. W. Moon.** 2002. Intimin facilitates colonization by *Escherichia coli* O157:H7 in adult ruminants. Infect. Immun. **70:**2704–2707.
5. **Dahan, S., S. Wiles, R. M. La Ragione, A. Best, M. J. Woodward, M. P. Stevens, R. K. Shaw, Y. Chong, S. Knutton, A. Phillips, and G. Frankel.** 2005. EspJ is a prophage-carried type III effector protein of attaching and effacing pathogens that modulates infection dynamics. Infect. Immun. **73:** 679–686.
6. **Datsenko, K. A., and B. L. Wanner.** 2000. One-step inactivation of chromosomal genes in *Escherichia coli* K-12 using PCR products. Proc. Natl. Acad. Sci. USA **97:**6640–6645.
7. **Dean-Nystrom, E. A., B. T. Bosworth, H. W. Moon, and A. D. O'Brien.** 1998. *Escherichia coli* O157:H7 requires intimin for enteropathogenicity in calves. Infect. Immun. **66:**4560–4563.
8. **Deng, W., J. L. Puente, S. Gruenheid, Y. Li, B. A. Vallance, A. Vazquez, J. Barba, J. A. Ibarra, P. O'Donnell, P. Metalnikov, K. Ashman, S. Lee, D. Goode, T. Pawson, and B. B. Finlay.** 2004. Dissecting virulence: systematic and functional analyses of a pathogenicity island. Proc. Natl. Acad. Sci. USA **101:**3597–3602.
9. **Dziva, F., P. M. van Diemen, M. P. Stevens, A. J. Smith, and T. S. Wallis.** 2004. Identification of *Escherichia coli* O157:H7 genes influencing colonization of the bovine gastrointestinal tract using signature-tagged mutagenesis. Microbiology **150:**3631–3645.
10. **Dziva, F., I. Vlisidou, V. F. Crepin, T. S. Wallis, G. Frankel, and M. P. Stevens.** 2007. Vaccination of calves with EspA, a key colonisation factor of *Escherichia coli* O157:H7, induces antigen-specific humoral responses but does not confer protection against intestinal colonisation. Vet. Microbiol. **123:**254–261.
11. **Garcia-Angulo, V. A., W. Deng, N. A. Thomas, B. B. Finlay, and J. L. Puente.** 2008. Regulation of expression and secretion of NleH, a new non-locus of enterocyte effacement-encoded effector in *Citrobacter rodentium*. J. Bacteriol. **190:**2388–2399.
12. **Garmendia, J., G. Frankel, and V. F. Crepin.** 2005. Enteropathogenic and enterohemorrhagic *Escherichia coli* infections: translocation, translocation, translocation. Infect. Immun. **73:**2573–2585.
13. **Garmendia, J., A. D. Phillips, M. F. Carlier, Y. Chong, S. Schuller, O. Marches, S. Dahan, E. Oswald, R. K. Shaw, S. Knutton, and G. Frankel.** 2004. TccP is an enterohaemorrhagic *Escherichia coli* O157:H7 type III effector protein that couples Tir to the actin-cytoskeleton. Cell. Microbiol. **6:**1167–1183.
14. **Girard, F., F. Dziva, P. van Diemen, A. D. Phillips, M. P. Stevens, and G. Frankel.** 2007. Adherence of enterohemorrhagic *Escherichia coli* O157, O26, and O111 strains to bovine intestinal explants ex vivo. Appl. Environ. Microbiol. **73:**3084–3090.
15. **Girard, F., I. P. Oswald, I. Taranu, P. Helie, G. D. Appleyard, J. Harel, and J. M. Fairbrother.** 2005. Host immune status influences the development of attaching and effacing lesions in weaned pigs. Infect. Immun. **73:**5514–5523.
16. **Gruenheid, S., I. Sekirov, N. A. Thomas, W. Deng, P. O'Donnell, D. Goode, Y. Li, E. A. Frey, N. F. Brown, P. Metalnikov, T. Pawson, K. Ashman, and B. B. Finlay.** 2004. Identification and characterization of NleA, a non-LEE-encoded type III translocated virulence factor of enterohaemorrhagic *Escherichia coli* O157:H7. Mol. Microbiol. **51:**1233–1249.
17. **Jarvis, K. G., J. A. Giron, A. E. Jerse, T. K. McDaniel, M. S. Donnenberg, and J. B. Kaper.** 1995. Enteropathogenic *Escherichia coli* contains a putative type III secretion system necessary for the export of proteins involved in attaching and effacing lesion formation. Proc. Natl. Acad. Sci. USA **92:**7996–8000.
18. **Jerse, A. E., J. Yu, B. D. Tall, and J. B. Kaper.** 1990. A genetic locus of enteropathogenic *Escherichia coli* necessary for the production of attaching and effacing lesions on tissue culture cells. Proc. Natl. Acad. Sci. USA **87:**7839–7843.
19. **Kenny, B., R. DeVinney, M. Stein, D. J. Reinscheid, E. A. Frey, and B. B. Finlay.** 1997. Enteropathogenic *E. coli* (EPEC) transfers its receptor for intimate adherence into mammalian cells. Cell **91:**511–520.
20. **Kim, D. W., G. Lenzen, A. L. Page, P. Legrain, P. J. Sansonetti, and C. Parsot.** 2005. The *Shigella flexneri* effector OspG interferes with innate immune responses by targeting ubiquitin-conjugating enzymes. Proc. Natl. Acad. Sci. USA **102:**14046–14051.
21. **Knutton, S., D. R. Lloyd, and A. S. McNeish.** 1987. Adhesion of enteropathogenic *Escherichia coli* to human intestinal enterocytes and cultured human intestinal mucosa. Infect. Immun. **55:**69–77.
22. **Lupp, C., M. L. Robertson, M. E. Wickham, I. Sekirov, O. L. Champion, E. C. Gaynor, and B. B. Finlay.** 2007. Host-mediated inflammation disrupts the intestinal microbiota and promotes the overgrowth of Enterobacteriaceae. Cell Host Microbe **2:**204.
23. **Marches, O., V. Covarelli, S. Dahan, C. Cougoule, P. Bhatta, G. Frankel, and E. Caron.** 2008. EspJ of enteropathogenic and enterohaemorrhagic *Escherichia coli* inhibits opsono-phagocytosis. Cell. Microbiol. **10:**1104–1115.
24. **Marches, O., T. N. Ledger, M. Boury, M. Ohara, X. Tu, F. Goffaux, J. Mainil, I. Rosenshine, M. Sugai, J. De Rycke, and E. Oswald.** 2003. Enteropathogenic and enterohaemorrhagic *Escherichia coli* deliver a novel effector called Cif, which blocks cell cycle G2/M transition. Mol. Microbiol. **50:**1553–1567.
25. **Marches, O., S. Wiles, F. Dziva, R. M. La Ragione, S. Schuller, A. Best, A. D. Phillips, E. L. Hartland, M. J. Woodward, M. P. Stevens, and G. Frankel.** 2005. Characterization of two non-locus of enterocyte effacement-encoded type III-translocated effectors, NleC and NleD, in attaching and effacing pathogens. Infect. Immun. **73:**8411–8417.
26. **McDaniel, T. K., K. G. Jarvis, M. S. Donnenberg, and J. B. Kaper.** 1995. A genetic locus of enterocyte effacement conserved among diverse enterobacterial pathogens. Proc. Natl. Acad. Sci. USA **92:**1664–1668.
27. **Mundy, R., F. Girard, A. J. FitzGerald, and G. Frankel.** 2006. Comparison of colonization dynamics and pathology of mice infected with enteropathogenic *Escherichia coli*, enterohaemorrhagic *E. coli* and *Citrobacter rodentium*. FEMS Microbiol. Lett. **265:**126–132.
28. **Mundy, R., T. T. MacDonald, G. Dougan, G. Frankel, and S. Wiles.** 2005. *Citrobacter rodentium* of mice and man. Cell. Microbiol. **7:**1697–1706.
29. **Mundy, R., L. Petrovska, K. Smollett, N. Simpson, R. K. Wilson, J. Yu, X. Tu, I. Rosenshine, S. Clare, G. Dougan, and G. Frankel.** 2004. Identification of a novel *Citrobacter rodentium* type III secreted protein, EspI, and roles of this and other secreted proteins in infection. Infect. Immun. **72:**2288–2302.
30. **Mundy, R., D. Pickard, R. K. Wilson, C. P. Simmons, G. Dougan, and G. Frankel.** 2003. Identification of a novel type IV pilus gene cluster required for gastrointestinal colonization of *Citrobacter rodentium*. Mol. Microbiol. **48:**795–809.
31. **Nataro, J. P., and J. B. Kaper.** 1998. Diarrheagenic *Escherichia coli*. Clin. Microbiol. Rev. **11:**142–201.
32. **Ruchaud-Sparagano, M. H., M. Maresca, and B. Kenny.** 2007. Enteropathogenic *Escherichia coli* (EPEC) inactivate innate immune responses prior to compromising epithelial barrier function. Cell. Microbiol. **9:**1909–1921.
33. **Stevens, M. P., A. J. Roe, I. Vlisidou, P. M. van Diemen, R. M. La Ragione, A. Best, M. J. Woodward, D. L. Gally, and T. S. Wallis.** 2004. Mutation of *toxB* and a truncated version of the *efa-1* gene in *Escherichia coli* O157:H7 influences the expression and secretion of locus of enterocyte effacement-encoded proteins but not intestinal colonization in calves or sheep. Infect. Immun. **72:**5402–5411.
34. **Tobe, T., S. A. Beatson, H. Taniguchi, H. Abe, C. M. Bailey, A. Fivian, R. Younis, S. Matthews, O. Marches, G. Frankel, T. Hayashi, and M. J. Pallen.** 2006. An extensive repertoire of type III secretion effectors in *Escherichia coli* O157 and the role of lambdoid phages in their dissemination. Proc. Natl. Acad. Sci. USA **103:**14941–14946.
35. **Tzipori, S., H. Karch, K. I. Wachsmuth, R. M. Robins-Browne, A. D. O'Brien, H. Lior, M. L. Cohen, J. Smithers, and M. M. Levine.** 1987. Role of a 60-megadalton plasmid and Shiga-like toxins in the pathogenesis of infection caused by enterohemorrhagic *Escherichia coli* O157:H7 in gnotobiotic piglets. Infect. Immun. **55:**3117–3125.
36. **van Diemen, P. M., F. Dziva, M. P. Stevens, and T. S. Wallis.** 2005. Identification of enterohemorrhagic *Escherichia coli* O26:H− genes required for intestinal colonization in calves. Infect. Immun. **73:**1735–1743.
37. **Vlisidou, I., F. Dziva, R. M. La Ragione, A. Best, J. Garmendia, P. Hawes, P. Monaghan, S. A. Cawthraw, G. Frankel, M. J. Woodward, and M. P. Stevens.** 2006. Role of intimin-Tir interactions and the Tir-cytoskeleton coupling protein in the colonization of calves and lambs by *Escherichia coli* O157:H7. Infect. Immun. **74:**758–764.
38. **Vlisidou, I., O. Marches, F. Dziva, R. Mundy, G. Frankel, and M. P. Stevens.** 2006. Identification and characterization of EspK, a type III secreted effector protein of enterohaemorrhagic *Escherichia coli* O157:H7. FEMS Microbiol. Lett. **263:**32–40.
39. **Whale, A. D., R. T. Hernandes, T. Ooka, L. Beutin, S. Schuller, J. Garmendia, L. Crowther, M. A. Vieira, Y. Ogura, G. Krause, A. D. Phillips, T. A. Gomes, T. Hayashi, and G. Frankel.** 2007. TccP2-mediated subversion of actin dynamics by EPEC 2—a distinct evolutionary lineage of enteropathogenic *Escherichia coli*. Microbiology **153:**1743–1755.
40. **Wiles, S., S. Clare, J. Harker, A. Huett, D. Young, G. Dougan, and G. Frankel.** 2004. Organ specificity, colonization and clearance dynamics in vivo following oral challenges with the murine pathogen *Citrobacter rodentium*. Cell. Microbiol. **6:**963–972.
41. **Wiles, S., K. M. Pickard, K. Peng, T. T. MacDonald, and G. Frankel.** 2006. In vivo bioluminescence imaging of the murine pathogen *Citrobacter rodentium*. Infect. Immun. **74:**5391–5396.
42. **Woodward, M. J., A. Best, K. A. Sprigings, G. R. Pearson, A. M. Skuse, A. Wales, C. M. Hayes, J. M. Roe, J. C. Low, and R. M. La Ragione.** 2003. Non-toxigenic *Escherichia coli* O157:H7 strain NCTC12900 causes attaching-effacing lesions and eae-dependent persistence in weaned sheep. Int. J. Med. Microbiol. **293:**299–308.

Editor: A. J. Bäumler